

Matching of Wilson loop eigenvalue densities in 1+1, 2+1 and 3+1 dimensions

Francis Bursa^a

^a*Institut für Theoretische Physik, Universität Regensburg, 93040 Regensburg, Germany*

Abstract

We investigate the matching of eigenvalue densities of Wilson loops in $SU(N)$ lattice gauge theory: the eigenvalue densities in 1+1, 2+1 and 3+1 dimensions are nearly identical when the traces of the loops are equal. We show that the matching is present to at least second order in the strong-coupling expansion, and also to second order in perturbation theory. We find that in the continuum limit there is matching at all values of the trace for bare Wilson loops. We confirm numerically that there is matching in these limits and find there are small violations away from them. We discuss the implications for the bulk transitions and for non-analytic gap formation at $N = \infty$ in 2+1 and 3+1 dimensions.

1 Introduction

The eigenvalues of an $SU(N)$ matrix are pure phases, $e^{i\alpha}$, and are gauge invariant for a closed Wilson loop. In [1] the eigenvalue distributions of Wilson loops in $D = 1 + 1$ and $D = 2 + 1$ $SU(N)$ lattice gauge theories were studied, and a remarkable result was found: if the eigenvalue distributions of Wilson loops $U_w^{n \times n}$ of size $n \times n$ were calculated in D and D' dimensions, with the couplings β_D and $\beta_{D'}$ chosen so that the expectation values of the traces in the fundamental representation $u_w^{n \times n} = \frac{1}{N} \text{ReTr}_F \{U_w^{n \times n}\}$ were equal,

$$\langle u_w^{n \times n}(\beta_D) \rangle_D = \langle u_w^{n \times n}(\beta_{D'}) \rangle_{D'}, \quad (1)$$

then the two eigenvalue distributions would match. This was found to apply over a wide range of couplings, loop sizes, and values of N . Preliminary results showed that the matching also applied to 3+1 dimensions. Matching between eigenvalue distributions in 1+1 and 3+1 dimensions was also found in [2] for $SU(2)$. The eigenvalue distribution of *smear*d Wilson loops in 3+1 dimensions in the large- N limit appears to approach the $D = 1 + 1$ $SU(\infty)$ distribution [3], suggesting the matching may also work for smeared loops, at least at $N = \infty$. An approximate matching of smeared Wilson loops between 1+1 and 3+1 dimensions has also been observed in $SU(2)$ [4].

If the matching found in [1] is exact it will have implications for the 2+1 dimensional and 3+1 dimensional theories. Firstly, in 1+1 dimensional lattice gauge theory there is the Gross-Witten transition [5] at $N = \infty$. This is a third-order phase transition which occurs when the trace of the plaquette is 0.5. At the transition a gap opens in the plaquette eigenvalue density. That is, on the strong-coupling side of the transition, the eigenvalue density is non-zero for all α , but on the weak-coupling side it is only non-zero for some range of angles $-\alpha_c < \alpha < \alpha_c$ with $\alpha_c < \pi$. If the matching is exact this gap opening, and hence the Gross-Witten transition, would be reproduced in 2+1 and 3+1 dimensions. In 2+1 dimensions there is a bulk transition at this value of the trace which is however different to the Gross-Witten transition, having a specific heat peak which is not present in 1+1 dimensions [1], so if the Gross-Witten transition is present it would have hidden in some way by this transition. Similarly in 3+1 dimensions there is a strong first-order bulk transition at $N = \infty$ (in fact for all $N \geq 5$) [6, 7, 8], which would have to hide the Gross-Witten transition.

Secondly, in 1+1 dimensional $SU(\infty)$ gauge theory in the continuum there is a non-analyticity, the Durhuus-Olesen transition, where a gap opens in the Wilson loop eigenvalue distribution at a critical Wilson loop area A_{crit} [9, 10]. If the matching is exact such a non-analyticity would also have to be present in the $D = 2 + 1$ and $D = 3 + 1$ cases. In the latter case, and if it occurs at a finite physical lengthscale, it could provide an explanation for the rapid crossover between perturbative and non-perturbative physics that is observed in the strong interactions [11, 12, 13]. It has also been suggested [3] that the non-analyticity at $N = \infty$ could be used to match perturbative and non-perturbative physics and thus calculate the string tension in terms of Λ_{QCD} .

However, exact matching would also imply that Casimir Scaling [14], which is exact in 1+1 dimensions, must also be exact in 2+1 and 3+1 dimensions. Casimir Scaling has been found to be a good approximation for tensions between sources in various representations of

$SU(3)$ in 3+1 dimensions [15, 16], but it is known not to be exact. It is also not exact for k -string tensions in both 2+1 and 3+1 dimensions [17]. Hence the matching cannot be exact, and must presumably be violated at some level.

The results in [1] were not the main purpose of that work and hence were somewhat limited; for example, the matching of traces in eq. (1) was not exact and there was no error analysis. The purpose of the present work is to carry out a more focused, quantitative study of the matching and of any violations that may be present, and to assess the implications for gap formation.

The structure of the paper is as follows: in the next section we show analytically that matching is present in both the strong-coupling and weak-coupling limits, and we consider the continuum limit. In Section 3 we present our numerical results. We conclude in Section 4.

2 Strong-coupling and weak-coupling limits

2.1 Strong coupling limit

The eigenvalue density of a Wilson loop $\rho(\alpha)$ can be expressed as a sum of Fourier components $F_k \cos(k\alpha)$. The Fourier coefficients F_k are just the traces of powers of the Wilson loop:

$$F_k = \frac{1}{N} \text{Re Tr}(W^k). \quad (2)$$

So if the traces of all powers of two Wilson loops are equal their eigenvalue densities will necessarily be equal too.

Consider the evaluation of such traces in the strong-coupling expansion for a planar Wilson loop of area A in lattice units. Apart from a possible constant term, the leading order contribution comes from the diagram in which we tile the Wilson loop with k sheets of plaquettes, giving a contribution proportional to $\langle u_p \rangle^{kA}$, where $\langle u_p \rangle$ is the trace of the plaquette. This is independent of the number of dimensions D , as are the group-theoretical prefactors. The trace in the fundamental representation is just $\langle u_p \rangle^A$, so the condition (1) is equivalent to matching the values of $\langle u_p \rangle$. Thus to leading order in the strong-coupling expansion we expect that the traces of all powers of the Wilson loops, and thus their eigenvalue distributions, will indeed match.

There is a possible loophole in this argument. The traces of powers of a Wilson loop can be reexpressed as combinations of traces of the Wilson loop in different irreducible representations. Some of these representations (for example the adjoint) can be screened in 2+1 and 3+1 dimensions, leading to a perimeter law instead of an area law. This should lead to violations of the matching. However, in practice what happens is that for small loops, the tiling with fewest plaquettes, which will give the leading term in the strong coupling expansion, is the one in which there are sheets of plaquettes tiling the plane of the loop, giving an area law. Tilings with sheets of plaquettes forming “tubes” around the outside of the loop, giving a perimeter law, only start to have fewer plaquettes for rather large loops. In the case of a square $L \times L$ loop, this will happen approximately when $L^2 = 16(L - 1)$, or at about $L = 15$. Such large

loops are difficult to study numerically, and in any case will have extremely small traces: if we are in strong coupling, so $\langle u_p \rangle < 0.4$, say, the trace in the fundamental representation of a 15×15 loop will be less than approximately $0.4^{15^2} \simeq 10^{-90}$. Traces in other representations will be even smaller. So the eigenvalue density will be indistinguishable from the Haar measure in practice, and there will trivially be matching between different dimensions.

Higher-order terms in the strong-coupling expansion do depend on the dimensionality of space-time, so we expect these to cause violations of the matching. The first such term is one in which one of the sheets of plaquettes tiling the Wilson loop has a “bump” in it. This involves an additional four plaquettes compared to tilings in which all the sheets are flat, so is suppressed by a factor $\langle u_p \rangle^4$. However, we show in Appendix A that in fact the contributions from the bump are identical in all dimensions when the traces are matched as in eq. (1).

So the first possible violations come in at the next order in the strong-coupling expansion. In $SU(2)$, the next order is tilings where one sheet has a “bump” in it, all the other sheets are flat, and there is an extra pair of plaquettes somewhere in one of the sheets. This is order $\langle u_p \rangle^{kA+6}$. In $SU(3)$ we must add three plaquettes instead of two, so the tiling is of order $\langle u_p \rangle^{kA+7}$, and for higher N we can add another “bump”, requiring an extra 4 plaquettes and giving tilings of order $\langle u_p \rangle^{kA+8}$.

These contributions are very small for all but the smallest loops. The largest contributions are those for $k = 2$ and for $SU(2)$. Assuming the prefactors to be of order one, and taking the largest $\langle u_p \rangle$ for which the strong-coupling expansion is valid to be approximately 0.4, these will be of order 0.001 for the plaquette, which should be easily observable, but only of order 10^{-6} for the 2×2 loop, which is unlikely to be detectable, and even smaller and hence almost certainly undetectable for larger loops. Thus we expect that when strong coupling applies, the eigenvalue densities of Wilson loops will be observed to match, except for the very smallest loops.

2.2 Weak coupling limit

We now consider the eigenvalue densities of Wilson loops in perturbation theory. As discussed in Section 2.1, if the traces of all powers of two Wilson loops are equal their eigenvalue densities will match. Furthermore, traces of powers of a Wilson loop can be expressed as combinations of traces of the Wilson loop in various representations. Thus to show that two Wilson loops will have matching eigenvalue densities it is sufficient to show that their traces in all representations are the same.

Wilson loops satisfy “Casimir Scaling” to second order in perturbation theory; that is, the trace of a Wilson loop in a representation R is given by

$$\frac{1}{N} \text{Tr}_R W = e^{-C_R f_D(g^2)}, \quad (3)$$

where C_R is the quadratic Casimir for the representation R , and $f_D(g^2)$ is a representation-independent function (which can however depend on the dimension of space-time D).

If eq. (1) is satisfied it is clear the *values* of the functions f_D and $f_{D'}$ must match. Then it follows that the traces in all other representations will match and hence the eigenvalue spectra

will match also.

Thus it seems that we expect matching when the coupling constant g^2 is sufficiently small that second-order perturbation theory is a good approximation. However, there is a subtlety involving representations with numerically large Casimirs C_R . These can be important when g^2 is small since then the trace of the Wilson loop approaches 1 so the eigenvalue distribution must be narrow. Then Fourier components with large k , that is traces of large powers of the Wilson loop, are important, and these can in general involve representations with large C_R . Now consider the trace of the Wilson loop in such a representation to leading order in perturbation theory:

$$\frac{1}{N} \text{Tr}_R W = 1 - W_1 C_R g^2. \quad (4)$$

Here W_1 is a representation-independent constant which depends on the Wilson loop size and the dimension D . If C_R is large the quadratic term in (4) can also be large even though g^2 is small. Then we expect that higher-order terms in perturbation theory could also be large, including those which violate Casimir Scaling at third order and higher.

However, consider the next term in the expansion of $\text{Tr}_R W$. This is of the form:

$$\frac{1}{N} \text{Tr}_R W = 1 - W_1 C_R g^2 + \left(\frac{1}{2} W_1^2 C_R^2 - W_2 C_R \right) g^4. \quad (5)$$

In the limit of very large C_R the quartic piece is dominated by the $\frac{1}{2} W_1^2 C_R^2 g^4$ term. This term comes from the exponentiation of the tree-level term $W_1 C_R g^2$:

$$e^{-W_1 C_R g^2} = 1 - W_1 C_R g^2 + \frac{1}{2} W_1^2 C_R^2 g^4 + \mathcal{O}(g^6). \quad (6)$$

The exponential will contribute a piece proportional to C_R^n to the g^{2n} term in the perturbation expansion. If the remaining parts of the g^{2n} term are lower order in C_R , as is the case for the g^2 and g^4 terms, the pieces coming from the exponential will dominate. The higher-order terms are not known, but if this is the case to all orders in g^2 , which seems plausible, the trace of the Wilson loop will be dominated by a term of the form (3) and there will be Casimir Scaling, and hence matching of the eigenvalue densities.

In the particular case of $N = \infty$ there is another argument for matching in perturbation theory which does not depend on the behaviour of representations with large Casimirs. For sufficiently weak coupling the eigenvalues are all near unity and then they will plausibly be in the same universality class as the Gaussian Unitary Ensemble, and so the density will be a ‘‘Wigner semicircle’’. This will be true in all dimensions, again leading to matching.

2.3 Continuum limit

The strong-coupling analysis in Section 2.1 applies when the lattice coupling constant, $\beta = \frac{2N}{g^2}$, is sufficiently small. This is the exact opposite of the continuum limit, for which we take β to infinity, so we do not expect the analysis to be useful in the continuum limit. Specifically, we expect that strong-coupling will apply below some critical coupling β_c . The trace of a Wilson loop of area A is approximately $\langle u_p \rangle^A$, where $\langle u_p \rangle \propto \beta$ is the trace of the plaquette. Hence

we expect the strong-coupling analysis to apply only for traces less than β_c^A , which indeed rapidly goes to zero in the continuum limit.

In 1+1 dimensions in the continuum Wilson loops obey an exact area law, $\langle u_w \rangle = e^{-\sigma a^2 L^2}$, where σ is the string tension, a is the lattice spacing, and L is the size of the loop in lattice units. So the boundary of the regime in which the weak-coupling analysis in Section 2.2 applies corresponds to a finite value of the trace. However, this is not the case in either 2+1 or 3+1 dimensions. In both these cases there is a “perimeter term”, due to the self-energy of the sources which propagate around the perimeter of the loop. The leading correction to $\ln\langle u_w \rangle$ is $aLV(a)$, where $V(r)$ is the Coulomb potential, which is proportional to $g^2 N \ln(r)$ and $g^2 N/r$ in $D = 2 + 1$ and $D = 3 + 1$ respectively. Combining this correction with the area term, we get

$$\langle u_w \rangle \propto \begin{cases} \exp(-caLg^2N \ln(ag^2N) - \sigma a^2 L^2) & D = 2 + 1 \\ \exp(-cg^2NL - \sigma a^2 L^2) & D = 3 + 1 \end{cases} \quad (7)$$

We see that in both cases if we take the continuum limit, keeping aL fixed, at a constant value of the coupling g^2N , the trace will decrease. So the boundary of the weak-coupling regimes will shift to lower traces in the continuum limit. This will happen only logarithmically in $D = 2 + 1$, but linearly in $D = 3 + 1$.

On the weak-coupling side of this boundary the traces of the Wilson loop in different representations will obey Casimir Scaling. But in $D = 1 + 1$ there is Casimir Scaling at all couplings, not just in weak-coupling. And by the arguments of Section 2.2, Casimir Scaling implies matching, so as long as we are on the weak-coupling side of the boundary there will be matching with loops in 1+1 dimensions. For sufficiently large L the minimum trace for which the coupling is weak will become arbitrarily small, and there should be matching at *all* values of the trace.

3 Results

3.1 Preliminaries

We discretise D -dimensional Euclidean space-time to a periodic cubic lattice with lattice spacing a and size L^D in lattice units. We assign $SU(N)$ matrices, U_l , to the links l of the lattice. We use the standard Wilson plaquette action

$$S = \beta \sum_p \left\{ 1 - \frac{1}{N} \text{ReTr} U_p \right\} \quad (8)$$

where U_p is the ordered product of the $SU(N)$ link matrices around the boundary of the plaquette p . We simulate the theory using a conventional mixture of heat bath and over-relaxation steps applied to the $SU(2)$ subgroups of the $SU(N)$ link matrices.

As discussed above, we expect that matching of eigenvalue spectra will only occur in certain limits. Specifically we expect to see matching in the strong-coupling limit, and when

the physical size of the loops is small enough that second-order perturbation theory is valid. As discussed in Section 2.3, due to the “perimeter term” this will be the case for loops with any finite trace in the continuum limit in both $D = 2 + 1$ and $D = 3 + 1$. So we expect to see matching for any value of the trace in the continuum limit also.

Thus we expect that, for each N , the part of parameter space in which matching does not occur will be constrained on three sides: in the direction of decreasing trace by strong coupling, in the direction of increasing trace by perturbation theory, and in the direction of increasing Wilson loop size (in lattice units) by the perimeter term. A fourth constraint is given by the loop size, which of course cannot become negative. Our strategy will be to determine for each Wilson loop size whether there is indeed a range of traces where matching does not occur, bounded by the strong-coupling regime on one side and the weak-coupling regime on the other, and then to increase the Wilson loop size to check whether this region moves to lower values of the trace, as expected due to the perimeter term.

We begin our investigation in $SU(2)$ since it is easiest to obtain the large statistics necessary to detect small violations there. We then turn to $SU(3)$ and $SU(6)$, to look at how things change with increasing N and, in the latter case, to investigate possible effects due to the first-order bulk transition which is present in $D = 3 + 1$ [6, 7, 8]. These calculations will allow us to draw some conclusions about what happens at $N = \infty$, and in particular whether the Gross-Witten and Durhuus-Olesen transitions will be reproduced there.

To perform a comparison for a particular loop size n at a particular value of the trace $\langle u_w \rangle$ we first generate configurations at couplings β_{run} in $D = 1 + 1$, $D = 2 + 1$, and $D = 3 + 1$. We then reweight to couplings β_{rew} where the traces match the target value of the trace exactly. On every sweep we calculate Wilson loops on every 1 to 2 lattice sites, and extract their eigenvalues. We store these in a histogram with a large number n_{bin} (typically 4096) of bins.

From these histograms we estimate the first $\frac{n_{\text{bin}}}{2}$ Fourier components F_k , defined by $F_k = \frac{1}{N} \sum_{i=1}^N \cos(k\alpha_i)$ where $\lambda_i = e^{i\alpha_i}$ is the i 'th eigenvalue, and the first $\frac{n_{\text{bin}}}{2}$ moments μ_k of the eigenvalue distribution. The finite width of the histogram bins means that these estimates will have errors of $\mathcal{O}\left(\frac{k^2}{n_{\text{bin}}}\right)$. As we shall see below, the relevant values of k are usually in the range 2 to 20, for which this is $\sim 10^{-5}$ and hence negligible. We compare the Fourier components and the moments of the eigenvalue distributions, searching for any statistically significant differences between the two distributions. We also compare the two histograms directly. To reduce the noise we also construct coarser histograms with $\frac{n_{\text{bin}}}{2}, \frac{n_{\text{bin}}}{4}, \dots, 4$ bins, and compare these.

Of course, these channels in which violations can show up are not independent; a generic violation will give a signal in all of them. What we find in practice is that the Fourier components are the most sensitive. That is, as we increase the statistics (at a loop size and trace for which we expect to see a violation), we first see a statistically significant difference in the Fourier components, and only for higher levels of statistics do the differences in the moments and histograms become significant. Thus from here on we will concentrate on our results for the Fourier components.

Furthermore, there is also a pattern in which Fourier components show significant differences first. We find that in $SU(2)$, a graph of the Fourier coefficients F_k typically looks like

that shown in Fig. 1: F_0 is always 1 by definition, F_1 is the trace and is always positive, and for larger k there is a rapid decrease in F_k to some maximally negative value, followed by an asymptotic approach to zero. We find that the Fourier components where significant differences first show up are those around the minimum. This is perhaps not surprising; it is easier to observe a small absolute difference if the quantity being observed is large. If the Fourier component is large and positive it is not far from 1 and thus largely perturbative. In this case we expect that we will not see any violations, as we discussed in Section 2.2. So indeed we expect that violations should be easiest to see for the Fourier components which are large and negative.

For larger N the graph of Fourier components F_k has more maxima and minima; we then find significant differences first appear in the Fourier components around the first minimum. We will refer to the value of k at which the first minimum in F_k occurs as k' . The corresponding Fourier component is then $F_{k'}$. Since the significant differences first appear in the Fourier components around the first minimum $F_{k'}$ is a useful quantity to use as a measure of the size of the violations, if any.

3.2 $SU(2)$

We now turn to our results, starting with those for $SU(2)$. Presumably violations of eigenvalue spectrum matching will be largest when we are furthest from the limits analysed in Section 2 where we expect matching. This leads us to look at small loops at moderate values of the trace. We begin with the smallest loop, the plaquette.

Our results for the plaquette are summarised in Table 1. We see that, as found in [1], the eigenvalue distributions in different numbers of dimensions when the traces are matched are indeed very similar. We illustrate this in Fig. 2, where we plot the plaquette eigenvalue densities at $\langle u_p \rangle = 0.7$, where the differences are largest. Despite this, we see that the differences are barely visible by eye. Turning to the Fourier components, which we plot in Fig. 3, we see that the differences are slightly more clear, but still extremely small. Note that these are the largest differences we see; at most values of the trace the differences would be impossible to see on such plots.

We see that, as discussed at the end of Section 3.1, the largest differences in Fig. 3 are around the Fourier component at the minimum, $F_{k'}$. To investigate how the differences vary with the trace $\langle u_p \rangle$, we plot in Fig. 4 the differences in $F_{k'}$ between 1+1 and 2+1 dimensions and between 1+1 and 3+1 dimensions, as a function of the trace.

Proceeding from small to large values of the trace, we see first of all that there are no detectable violations at $\langle u_p \rangle = 0.07$, where the coupling is very strong. Violations become visible, possibly at $\langle u_p \rangle = 0.3$, and certainly at $\langle u_p \rangle = 0.4$, still within the strong-coupling region. After this they rapidly increase, reaching a maximum when the trace is around 0.8 for the difference between 1+1 and 2+1 dimensions and 0.6–0.7 for the difference between 1+1 and 3+1 dimensions. Finally they decrease again as we approach $\langle u_p \rangle = 1$. We see the same features for other values of k near k' , and also (though with relatively larger statistical errors) for the moments and histograms of the distributions.

All this is as we would expect. There is a large range of traces in strong coupling for

which there are no observable violations of the matching. Violations start to appear around the upper limit of strong coupling, due to the higher-order terms in the strong-coupling expansion (though they are smaller than we estimated; presumably the prefactors are small). Then there is an intermediate-coupling region where there is no reason to expect matching and where we indeed see violations. Finally the coupling becomes weak and the matching reappears due to Casimir Scaling.

For the larger values of the trace, the volumes used in $D = 2+1$ and especially in $D = 3+1$ are extremely small. Indeed, our calculations for $\langle u_p \rangle = 0.99$ in 3+1 dimensions were carried out at a coupling $\beta = 75.2$, for which the lattice spacing is $\sim 10^{-80}$ fm! Thus one might worry that the small differences we see there are not due to true infinite-volume differences between the theories but are instead due to finite-volume effects. To check for this, we have repeated our calculations on different sized lattices. We find no difference in the violations in matching as we change the lattice size, making it unlikely that these are finite-volume effects.

We now turn to our results for 2×2 Wilson loops. These are listed in Table 2, and the corresponding differences in $F_{k'}$ are plotted in Fig. 5. We can compare these to our results for the plaquette in Table 1 and Fig. 4. Proceeding from small to large traces, we see first of all that there are violations for 2×2 loops at much smaller values of the trace than for the plaquette. This is because the boundary of strong-coupling has shifted to a much smaller trace — indeed at $\langle u_w \rangle = 0.04$ the trace of the plaquette is 0.447, 0.444 and 0.438 in 1+1, 2+1 and 3+1 dimensions respectively, so we are already near the edge of strong coupling. The violations of matching are just becoming detectable here. They then become larger, as for the plaquette, but reach maxima and start decreasing at lower values of the trace than for the plaquette. This is presumably the effect of the perimeter term lowering the value of the trace at which weak-coupling begins. We see that the peak is shifted to a lower value of the trace in 3+1 dimensions compared to 2+1 dimensions, as expected since the perimeter term is stronger in the former case.

We also see that the magnitude of the violations is smaller by a factor of 5 or so compared to the plaquette. This is not just because of the perimeter term, which causes larger loops to be at a weaker coupling at the same value of the trace. For example, comparing the plaquette at a trace of 0.8 to the 2×2 Wilson loop at a trace of 0.5, we see the violations are much larger for the plaquette, despite the fact that the couplings are roughly the same. Presumably what is going on is that there are relatively large lattice corrections to Casimir Scaling for the plaquette, which spoil the matching, but these corrections are smaller for the 2×2 loop.

Finally we look at our results for 4×4 loops, which are listed in Table 3 and plotted in Fig. 6. We see that the difference between 1+1 and 2+1 dimensions is non-zero for much smaller values of the trace than for the smaller loops, as expected. For the difference between 1+1 and 3+1 dimensions the situation is less clear — the peak appears to be around $\langle u_w \rangle = 0.5$, as for 2×2 loops — but it is clear the violations are now extremely small.

Above we have described the behaviour of the Fourier component $F_{k'}$ for the 2×2 and 4×4 loops, but as for the plaquettes we see essentially the same behaviour for other Fourier components with k near k' , and for the moments and histograms of the eigenvalue densities.

3.3 $SU(3)$ and $SU(6)$

We now turn to our results for $SU(3)$ and $SU(6)$. Our results here are less extensive and are aimed mainly at establishing that the features we saw for $SU(2)$ carry over to larger N .

Our results for the plaquette in $SU(3)$ are summarised in Table 4 and are plotted in Fig. 7. We see a similar pattern to the corresponding results in $SU(2)$: there is very good matching at small values of the trace, followed by violations of the matching at intermediate values, which decrease again as we approach $\langle u_p \rangle = 1$. The violations appear to be somewhat larger than for $SU(2)$.

Our results for the plaquette in $SU(6)$ are summarised in Table 5 and are plotted in Fig. 8. Note that due to the bulk transition there is a range of $\langle u_p \rangle$ around 0.5 which is inaccessible in 3+1 dimensions; the closest we can get is $\langle u_p \rangle = 0.435$ and $\langle u_p \rangle = 0.52$ on the strongly-coupled and weakly-coupled sides respectively. The overall pattern of violations is similar to that for $SU(2)$ and $SU(3)$: again we have good matching at small and large values of the trace and violations in between. There is no sign of anything exceptional happening around $\langle u_p \rangle = 0.5$, the region where the bulk transitions occur.

The maximum violations now appear quite large (~ 0.02). To judge whether this is in fact large, we can compare the values of $F_{k'}$ at a trace of 0.5 in Tables 5 and 7. We see that they are around -0.04 for the plaquettes and -0.105 for the 2×2 loops, so distributions in which the $F_{k'}$ differ by ~ 0.06 are certainly possible. So the violations observed are still significantly smaller than they could be.

Our results for 2×2 loops are summarised in Tables 6 and 7 for $SU(3)$ and $SU(6)$ respectively. They are plotted in Figs. 9 and 10. Again, the pattern of violations is broadly similar to that seen in $SU(2)$, shown in Fig. 5. The biggest change is that the peak violations are larger and occur at a lower value of the trace in $SU(6)$. Why this should be is unclear; it occurs in the intermediate-coupling region where we do not have an analytic understanding of the source of the violations. In any case the violations are still small, and they decrease in both the strong-coupling and weak-coupling regions, as they should.

The differences described above are for the Fourier component $F_{k'}$, but we see the same patterns for nearby Fourier components and for the moments and histograms.

In summary, we see that despite some differences in the details, the violations in $SU(3)$ and $SU(6)$ follow the same broad patterns as in $SU(2)$, and are consistent with our expectations based on strong-coupling and weak-coupling analysis.

4 Conclusions

We have shown that the remarkable matching between eigenvalue spectra of Wilson loops observed in [1, 2, 3, 4] can be understood analytically in both the strong-coupling and weak-coupling limits. In the strong-coupling limit, it follows from the fact that the leading-order contributions come from tilings that are flat, and hence the same, in all dimensions. In the weak-coupling limit it follows from the fact that Wilson loops satisfy Casimir Scaling up to second order in perturbation theory in all dimensions. Due to the “perimeter term”,

perturbation theory applies at all values of the trace in the continuum limit, so the matching will apply there also.

However, our numerical results have shown that away from these limits the matching of eigenvalue densities is not exact. These differences remain small, of order 0.02 at most. Why this should be when we are well away from both the strong-coupling and weak-coupling regimes is unclear.

Apart from their small size, the overall pattern of violations follows our expectations: it approaches zero in both the strong-coupling and weak-coupling limits, and has a peak at intermediate couplings. The trace at which this peak occurs decreases as the size of the loop increases, as expected due to the effect of the perimeter term.

In the large- N limit in 1+1 dimensions, the Gross-Witten transition occurs when the trace of the plaquette is 0.5 [5]. At this value of the trace we observe finite differences between the eigenvalue densities in 1+1 and 2+1 dimensions which show no sign of decreasing (indeed, they appear to increase) with N . This implies that the Gross-Witten transition will not be reproduced in $D = 2 + 1$, which is consistent with the results found in [1], where a peak was observed in the specific heat at the bulk transition in 2+1 dimensions which is not present at the Gross-Witten transition.

In 3+1 dimensions a jump in the trace of the plaquette occurs at the bulk transition making values around 0.5 inaccessible. However, we see differences in the eigenvalue densities on either side of this jump, suggesting that even if the bulk transition was removed there would still be significant differences at a trace of 0.5 and thus any “underlying” transition would again be different to the Gross-Witten transition.

The situation is different for the Durhuus-Olesen non-analyticity in Wilson loop eigenvalue densities which occurs at $N = \infty$ in the continuum in 1+1 dimensions [9, 10]. This occurs when the trace of the Wilson loop is $e^{-2} \approx 0.135$. Due to the perimeter term this will be in the weak-coupling limit in the continuum limit, where we expect matching. Thus we expect that the non-analyticity will be reproduced in both 2+1 and 3+1 dimensions. However, since it occurs in the weak-coupling limit it is in the far ultraviolet, so it seems unlikely to be physically significant.

This problem could be avoided by using smeared, instead of bare, Wilson loops, as was done in [3, 4]. If the perimeter term was eliminated completely by smearing the Wilson loops would have a trace of e^{-2} at a constant lengthscale in physical units in the continuum limit (although the lengthscale would be determined by the details of the smearing procedure). However, the Wilson loops would then be given completely by the area term, which does not satisfy Casimir Scaling exactly in 2+1 or 3+1 dimensions. Then the traces of Wilson loops in different representations will not match and so neither will the eigenvalue densities, and so the non-analyticity in $D = 1 + 1$ will *not* be reproduced for smeared Wilson loops in 2+1 or 3+1 dimensions.

We still expect gap formation to occur, since the eigenvalue density becomes flat as $u_w \rightarrow 0$ on the one hand, and forms a Wigner semicircle as $u_w \rightarrow 1$ on the other. In between a gap must form. However, since the lengthscale it will occur at will depend on the details of the smearing procedure, it is unclear whether the gap formation will have any physical significance. Also, since the eigenvalue density will be different from that at the Durhuus-Olesen non-

analyticity, it is not clear what universality class the gap formation will fall into. This is a question that needs to be resolved in order to implement the idea of matching perturbative and non-perturbative physics through the transition, as set out in [3].

In summary, we have understood the matching of Wilson loop eigenvalue densities in both the strong-coupling and weak-coupling limits, and shown it is violated away from these limits. These violations imply that the Gross-Witten transition will not be matched in 2+1 and 3+1 dimensions. The Durhuus-Olesen non-analyticity will be reproduced for bare loops in 2+1 and 3+1 dimensions, but at an ultraviolet length-scale, and it will not be reproduced for smeared loops.

Acknowledgments

We are grateful to Mike Teper for many useful discussions throughout this work. This work was supported by the EC Hadron Physics I3 Contract RII3-CT-2004-506078 and by the BMBF.

A Matching of eigenvalue spectra in the strong-coupling expansion

As shown in Section 2.1, matching the traces of two Wilson loops according to eq. (1) leads to matching of the traces of all powers of the loops, and hence to matching of the spectra, to leading order in the strong-coupling expansion. In this Appendix we consider the next order, described by tilings with one “bump”, and show that the matching also works there.

We consider first the plaquette in $SU(2)$. The strong-coupling expansion for the trace in $D = 1 + 1$ dimensions is

$$\text{Tr}(P) = a_1\beta_1 + a_3\beta_1^3 + a_5\beta_1^5 + \mathcal{O}(\beta_1^7), \quad (9)$$

and in $D' = 2 + 1, 3 + 1$ dimensions it is

$$\text{Tr}(P) = a_1\beta_{D'} + a_3\beta_{D'}^3 + b_5\beta_{D'}^5 + \mathcal{O}(\beta_{D'}^7). \quad (10)$$

The β and β^3 terms are the same in both cases since they correspond to only planar tilings, but the β^5 terms are different since they can include a “bump” in 2+1 or 3+1 dimensions.

Similarly, the strong-coupling expansion of the trace of the plaquette squared is

$$\text{Tr}(P^2) = c_2\beta_1^2 + c_4\beta_1^4 + c_6\beta_1^6 + \mathcal{O}(\beta_1^8) \quad (11)$$

in 1+1 dimensions, and

$$\text{Tr}(P^2) = c_2\beta_{D'}^2 + c_4\beta_{D'}^4 + d_6\beta_{D'}^6 + \mathcal{O}(\beta_{D'}^8) \quad (12)$$

in D' dimensions. The first term is $\mathcal{O}(\beta^2)$, rather than $\mathcal{O}(\beta)$, since we need to tile the doubly-winding loop with two plaquettes, the β^4 term has 4 plaquettes, the β^6 term has either 6 plaquettes in the plane or 1 in the plane and 5 in a bump, and so on.

The matching condition (1) is that (9) and (10) are equal. We can expand $\beta_{D'}$ in β_1 ; the condition gives

$$\beta_{D'} = \beta_1 + \frac{a_5 - b_5}{a_1} \beta_1^5 + \mathcal{O}(\beta_1^7). \quad (13)$$

Substituting this into (12) we find the values of $\text{Tr}(P^2)$ will match in 1+1 and D' dimensions if the coefficients in the expansion are related as follows:

$$d_6 = c_6 + 2 \frac{c_2}{a_1} (b_5 - a_5). \quad (14)$$

The first term on the right-hand side is the $\mathcal{O}(\beta_1^6)$ term in (11), which is the same as the contribution from flat tilings to d_6 . The second term should then give the contribution from tilings with a bump if (14) is to be satisfied. Now $b_5 - a_5$ is the difference between the $\mathcal{O}(\beta^5)$ contributions to (10) and (9) i.e. it is the contribution from a ‘‘bump’’ in a single sheet. The factor $\frac{c_2}{a_1}$ accounts for the different multiplicative factors we require when tiling a doubly-winding loop with two sheets rather than a singly-winding loop with one sheet. Finally the factor of 2 accounts for the fact that the ‘‘bump’’ can occur in either of the two sheets. Putting all these together gives exactly the correct expression for d_6 , so (14) is indeed satisfied.

Generalising this to the trace of the k 'th power of the Wilson loop $\text{Tr}(P^k)$ is straightforward. It is also straightforward to generalise to Wilson loops of area A . Finally, changing N changes the number of plaquettes we can add to a tiling at one site from 2 to N ; this will change the $\mathcal{O}(\beta^3)$ terms in (9) and (10) to $\mathcal{O}(\beta^{1+N})$, but it will not affect the ‘‘bump’’ contribution at $\mathcal{O}(\beta^5)$ since this is singly-tiled everywhere. Hence the proof above will also work for all values of N .

So the first term in the strong-coupling expansion corresponding to tilings in which one of the sheets has a ‘‘bump’’ will indeed give matching of traces of powers of the Wilson loop if the matching condition (1) is satisfied. Hence the eigenvalue densities will also match up to that order in the strong-coupling expansion.

References

- [1] F. Bursa and M. Teper, Phys. Rev. D74 (2006) 125010 [hep-lat/0511081].
- [2] T. Belova, Y. Makeenko, M. Polikarpov and A. Veselov, Nucl. Phys. B230[FS10] (1984) 473.
- [3] R. Narayanan and H. Neuberger, JHEP 0603 (2006) 064 [hep-th/0601210].
- [4] A. Brzoska, F. Lenz, J. Negele and M. Thies, Phys. Rev. D71 (2005) 034008 [hep-th/0412003].

- [5] D. Gross and E. Witten, Phys. Rev. D 21 (1980) 446.
- [6] M. Campostrini, Nucl. Phys. Proc. Suppl. 73 (1999) 724 [hep-lat/9809072].
- [7] B. Lucini and M. Teper, JHEP 0106 (2001) 050 [hep-lat/0103027].
- [8] B. Lucini, M. Teper and U. Wenger, JHEP 0502 (2005) 033 [hep-lat/0502003].
- [9] B. Durhuus and P. Olesen, Nucl. Phys. B184 (1981) 461.
- [10] A. Bassetto, L. Griguolo and F. Vian, Nucl. Phys. B559 (1999) 563 [hep-th/9906125].
- [11] M. Teper, hep-th/0412005.
- [12] R. Jaffe, Invited talk at ‘QCD and Strings’, ECT, July 2004.
- [13] R. Narayanan and H. Neuberger, PoS Lat2005 (2006) 005 [hep-lat/0509014].
- [14] J. Ambjørn, P. Olesen and C. Peterson, Nucl. Phys. B240 (1984) 533.
- [15] S. Deldar, Phys. Rev. D62 (2000) 034509 [hep-lat/9911008].
- [16] G. Bali, Phys. Rev. D62 (2000) 114503 [hep-lat/0006022].
- [17] B. Lucini and M. Teper, Phys. Rev. D64 (2001) 105019 [hep-lat/0107007].

Plaquette in $SU(2)$					
$\langle u_p \rangle$	Lattice size	β_{run}	β_{rew}	k'	$F_{k'}$
0.07	4^2	0.281	0.28095	2	-0.495066(20)
	4^3	0.2807	0.28078		-0.495087(13)
	4^4	0.2808	0.28082		-0.495087(8)
0.3	4^2	1.279	1.27893	2	-0.407127(32)
	4^3	1.2605	1.26049		-0.407189(37)
	4^4	1.242	1.24140		-0.407195(45)
0.4	4^2	1.803	1.80340	3	-0.351050(35)
	4^3	1.729	1.72878		-0.351121(18)
	4^4	1.648	1.64803		-0.351256(25)
0.5	4^2	2.444	2.44677	3	-0.39550(17)
	4^3	2.235	2.23511		-0.39629(7)
	4^4	1.996	1.99071		-0.39769(24)
0.6	8^2	3.31	3.3114	3	-0.39758(18)
	8^3	2.83	2.8279		-0.40010(14)
	8^4	2.29	2.2933		-0.40638(13)
0.7	8^2	4.64	4.6440	4	-0.40855(14)
	8^3	3.67	3.6734		-0.41185(6)
	8^4	2.804	2.8033		-0.41736(9)
0.8	8^2	7.17	7.1940	5	-0.41510(35)
	8^3	5.3	5.3006		-0.41921(14)
	8^4	4.0	4.0062		-0.42260(20)
0.9	8^2	14.7	14.719	7	-0.43006(34)
	8^3	10.27	10.253		-0.43298(17)
	8^4	7.73	7.729		-0.43448(15)
0.97	8^2	49.4	49.598	12	-0.44220(14)
	8^3	33.5	33.545		-0.44332(5)
	8^4	25.2	25.218		-0.44385(5)
0.99	12^2	149.01	149.534	21	-0.444903(84)
	12^3	100.15	100.211		-0.445286(19)
	12^4	75.2	75.194		-0.445457(33)

Table 1: Fourier components $F_{k'}$ at the minimum k' of the Fourier spectrum of the eigenvalue distribution, for plaquettes in $SU(2)$.

2×2 Wilson loops in $SU(2)$					
$\langle u_w \rangle$	Lattice size	β_{run}	β_{rew}	k'	$F_{k'}$
0.04	8^2	2.0883	2.08746	2	-0.499370(10)
	8^3	1.9434	1.94312		-0.499358(13)
	8^4	1.7915	1.79090		-0.499344(10)
0.07	8^2	2.555	2.55399	2	-0.497887(13)
	8^3	2.273	2.27472		-0.497781(18)
	8^4	1.985	1.98421		-0.497697(25)
0.15	12^2	3.552	3.55501	2	-0.487888(29)
	12^3	2.877	2.87655		-0.487604(24)
	12^4	2.233	2.23233		-0.487568(34)
0.3	12^2	5.438	5.4385	2	-0.435366(23)
	12^3	3.85	3.8501		-0.435169(22)
	12^4	2.646	2.6459		-0.436626(77)
0.4	12^2	7.019	7.0179	3	-0.376907(63)
	12^3	4.642	4.6417		-0.377007(39)
	12^4	3.119	3.1167		-0.377989(79)
0.5	12^2	9.13	9.1355	3	-0.43410(7)
	12^3	5.7	5.7104		-0.43470(8)
	12^4	3.8	3.8015		-0.43584(19)
0.6	12^2	12.22	12.2357	3	-0.44130(13)
	12^3	7.285	7.2886		-0.44210(8)
	12^4	4.82	4.8230		-0.44279(5)
0.7	12^2	17.3	17.3138	4	-0.43348(21)
	12^3	9.87	9.8833		-0.43417(14)
	12^4	6.54	6.5368		-0.43445(10)
0.8	12^2	27.39	27.3759	5	-0.432074(48)
	12^3	15.08	15.0791		-0.432562(47)
	12^4	9.97	9.9604		-0.432752(37)
0.9	16^2	57.36	57.4346	7	-0.439275(47)
	16^3	30.66	30.6838		-0.439529(36)
	16^4	20.23	20.2416		-0.439604(42)
0.97	24^2	197.5	197.411	12	-0.445541(25)
	24^3	103.5	103.483		-0.445624(14)

Table 2: Fourier components $F_{k'}$ at the minimum k' of the Fourier spectrum of the eigenvalue distribution, for 2×2 Wilson loops in $SU(2)$.

4 × 4 Wilson loops in $SU(2)$					
$\langle u_w \rangle$	Lattice size	β_{run}	β_{rew}	k'	$F_{k'}$
0.04	16^2	7.933	7.93321	2	-0.499699(10)
	16^3	4.497	4.49635		-0.499642(12)
	16^4	2.636	2.63619		-0.499688(9)
0.07	16^2	9.506	9.50617	2	-0.498705(8)
	16^3	5.067	5.06701		-0.498632(10)
	16^4	2.8908	2.89075		-0.498708(9)
0.2	16^2	15.4	15.4000	2	-0.479298(11)
	16^3	7.1843	7.18433		-0.479154(8)
	16^4	3.9905	3.99028		-0.479322(11)
0.4	16^2	26.69	26.6860	3	-0.379362(15)
	16^3	11.219	11.2183		-0.379351(18)
	16^4	6.231	6.23144		-0.379401(20)
0.5	16^2	35.124	35.1209	3	-0.437299(16)
	16^3	14.224	14.2245		-0.437275(17)
	24^4	7.9327	7.93339		-0.437364(12)
0.7	24^2	67.74	67.7909	4	-0.435227(19)
	24^3	25.974	26.0474		-0.435269(21)
	24^4	14.563	14.5656		-0.435259(16)

Table 3: Fourier components $F_{k'}$ at the minimum k' of the Fourier spectrum of the eigenvalue distribution, for 4×4 Wilson loops in $SU(2)$.

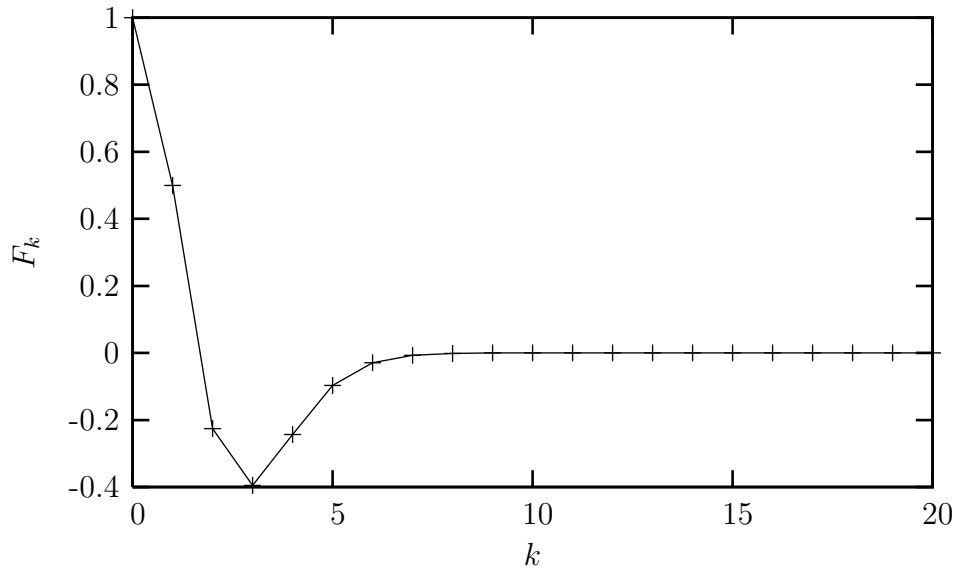


Figure 1: Fourier components F_k for the plaquette in $SU(2)$ with $\langle u_p \rangle = 0.5$ on a 4^2 lattice.

Plaquette in $SU(3)$					
$\langle u_p \rangle$	Lattice size	β_{run}	β_{rew}	k'	$F_{k'}$
0.07	4^2	1.15	1.15022	2	-0.062686(18)
	4^3	1.15	1.15038		-0.062663(25)
	4^4	1.152	1.15112		-0.062670(20)
0.3	4^2	4.268	4.2690	2	-0.165392(13)
	4^3	4.187	4.1864		-0.165408(13)
	4^4	4.102	4.1017		-0.165438(13)
0.5	4^2	7.3	7.2996	2	-0.11133(6)
	4^3	6.484	6.4920		-0.11246(9)
	4^4	5.51	5.4985		-0.11543(27)
0.7	8^2	12.94	12.9408	3	-0.16766(8)
	8^3	9.91	9.9328		-0.17274(6)
	8^4	7.54	7.5356		-0.17800(8)
0.97	8^2	132.8	132.798	11	-0.193903(31)
	8^3	89.6	89.597		-0.194490(31)
	8^4	67.4	67.338		-0.194797(34)

Table 4: Fourier components $F_{k'}$ at the minimum k' of the Fourier spectrum of the eigenvalue distribution, for plaquettes in $SU(3)$.

Plaquette in $SU(6)$					
$\langle u_p \rangle$	Lattice size	β_{run}	β_{rew}	k'	$F_{k'}$
0.3	4^2	20.78	20.7839	2	-0.031469(28)
	4^3	20.42	20.4343		-0.031658(51)
	4^4	20.09	20.0838		-0.031747(26)
0.435	4^2	29.7	29.355	2	-0.04909(4)
	4^4	24.45	24.451		-0.05650(12)
0.5	4^2	34.0	33.970	2	-0.03759(8)
	4^3	29.7	29.882		-0.04316(6)
0.52	4^2	35.5	35.575	2	-0.03020(8)
	4^4	24.15	24.129		-0.05103(24)
0.7	8^2	58.0	57.920	3	-0.09947(5)
	8^3	43.8	43.788		-0.10963(5)
	8^4	33.1	33.160		-0.11784(9)
0.97	8^2	582.3	582.73	10	-0.13828(11)
	8^3	391.0	391.28		-0.13952(7)
	8^4	294.2	294.59		-0.14012(7)

Table 5: Fourier components $F_{k'}$ at the first minimum k' of the Fourier spectrum of the eigenvalue distribution, for plaquettes in $SU(6)$.

2×2 Wilson loops in $SU(3)$					
$\langle u_w \rangle$	Lattice size	β_{run}	β_{rew}	k'	$F_{k'}$
0.04	8^2	6.39	6.3875	2	-0.03891(5)
	8^3	5.83	5.8241		-0.03887(7)
	8^4	5.22	5.2101		-0.03889(13)
0.15	12^2	10.12	10.1213	2	-0.130071(21)
	12^3	7.857	7.8574		-0.129931(46)
	12^4	5.774	5.7742		-0.130398(56)
0.5	12^2	24.86	24.8285	2	-0.14448(8)
	12^3	15.17	15.1684		-0.14497(13)
	12^4	10.1	10.1042		-0.14548(13)
0.9	12^2	153.5	153.412	6	-0.194108(25)
	12^3	81.7	81.767		-0.194218(56)
	12^4	53.97	53.959		-0.194307(62)

Table 6: Fourier components $F_{k'}$ at the minimum k' of the Fourier spectrum of the eigenvalue distribution, for 2×2 Wilson loops in $SU(3)$.

2×2 Wilson loops in $SU(6)$					
$\langle u_w \rangle$	Lattice size	β_{run}	β_{rew}	k'	$F_{k'}$
0.04	8^2	30.18	30.1791	2	-0.008415(31)
	8^3	27.47	27.4617		-0.008467(34)
	8^4	24.42	24.4228		-0.008630(52)
0.15	12^2	45.8	45.8021	2	-0.066150(48)
	12^3	34.8	34.8034		-0.067323(34)
	12^4	25.035	25.0292		-0.069585(53)
0.5	12^2	109.5	109.584	2	-0.10342(6)
	12^3	66.4	66.259		-0.10453(15)
	12^4	44.25	44.2464		-0.10534(13)
0.9	12^2	672.4	672.859	6	-0.137916(64)
	12^3	358.0	357.767		-0.138330(41)
	12^4	236.0	236.098		-0.138396(50)

Table 7: Fourier components $F_{k'}$ at the first minimum k' of the Fourier spectrum of the eigenvalue distribution, for 2×2 Wilson loops in $SU(6)$.

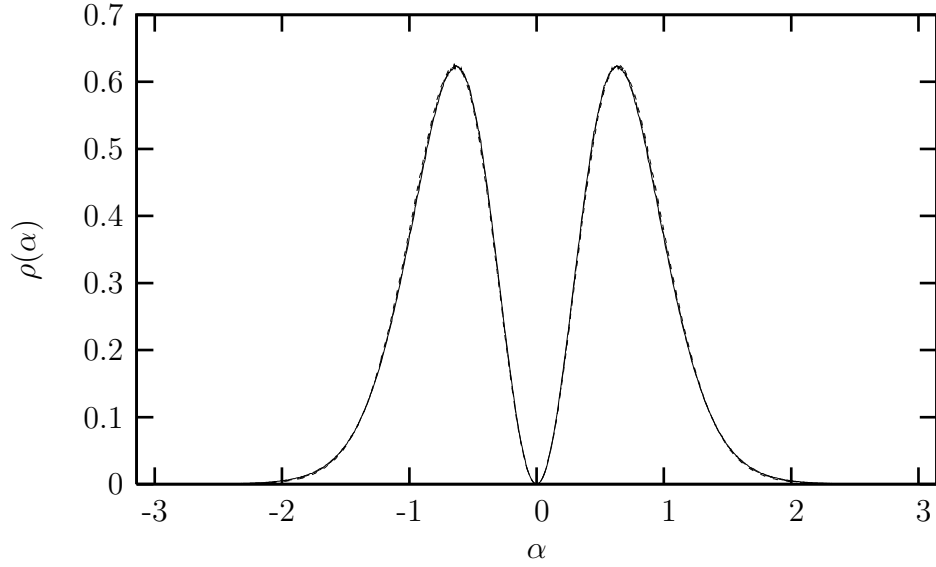


Figure 2: Eigenvalue densities for the plaquette in $SU(2)$ with $\langle u_p \rangle = 0.7$ in $D = 1 + 1$ (solid line), $D = 2 + 1$ (dashed) and $D = 3 + 1$ (dotted).

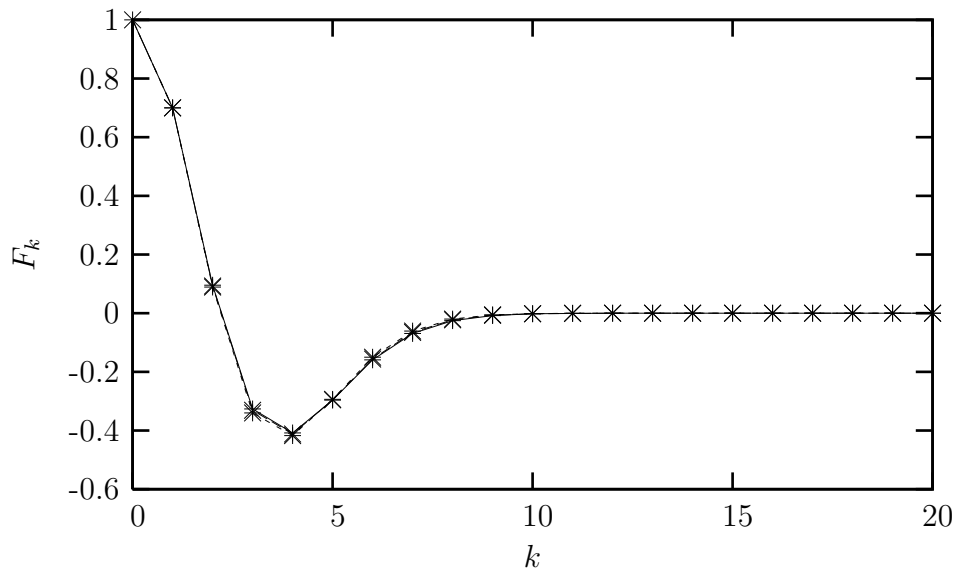


Figure 3: Fourier components F_k for the plaquette in $SU(2)$ with $\langle u_p \rangle = 0.7$ in $D = 1 + 1$ (+), $D = 2 + 1$ (x) and $D = 3 + 1$ (*).

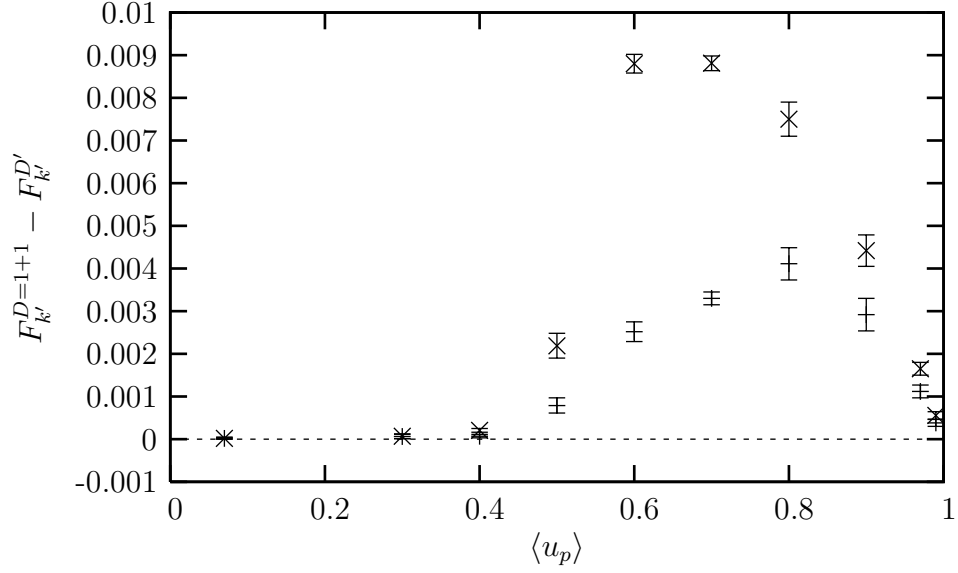


Figure 4: Difference between $F_{k'}$ in 1+1 dimensions and D' dimensions, for $D' = 2 + 1$ (+) and $D' = 3 + 1$ (\times), as a function of the trace $\langle u_p \rangle$. All for the plaquette in $SU(2)$.

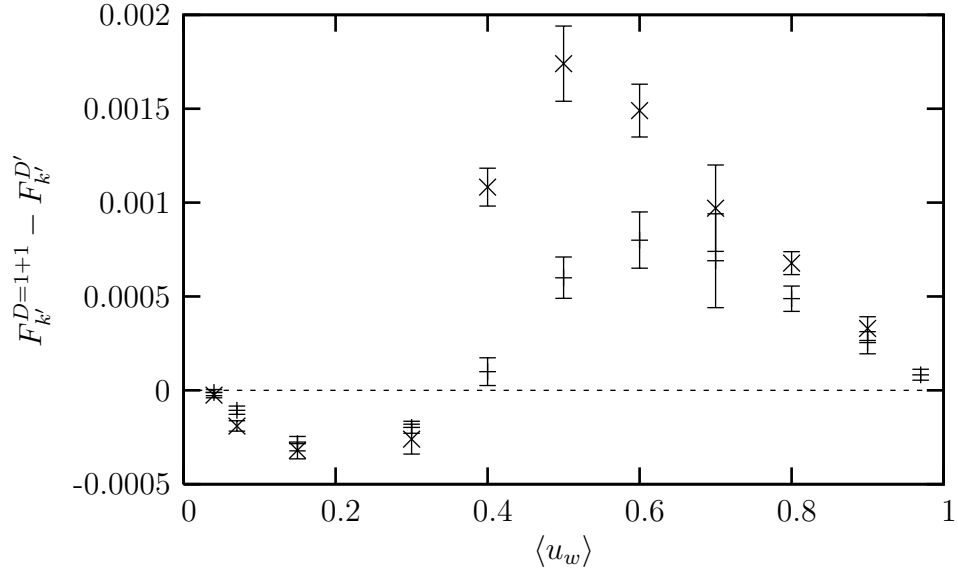


Figure 5: Difference between $F_{k'}$ in 1+1 dimensions and D' dimensions, for $D' = 2 + 1$ (+) and $D' = 3 + 1$ (\times), as a function of the trace $\langle u_w \rangle$. All for the 2×2 Wilson loop in $SU(2)$.

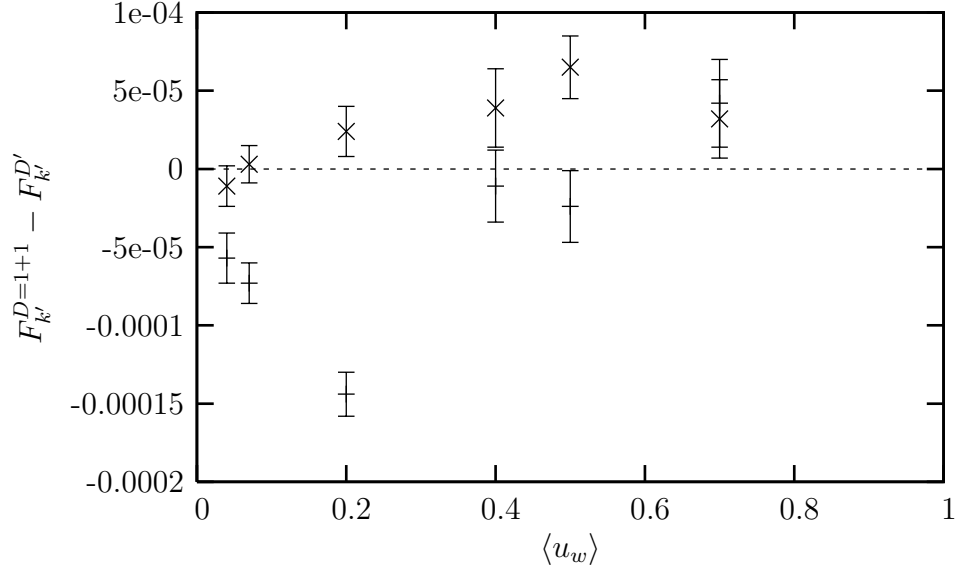


Figure 6: Difference between $F_{k'}$ in 1+1 dimensions and D' dimensions, for $D' = 2 + 1$ (+) and $D' = 3 + 1$ (x), as a function of the trace $\langle u_w \rangle$. All for the 4×4 Wilson loop in $SU(2)$.

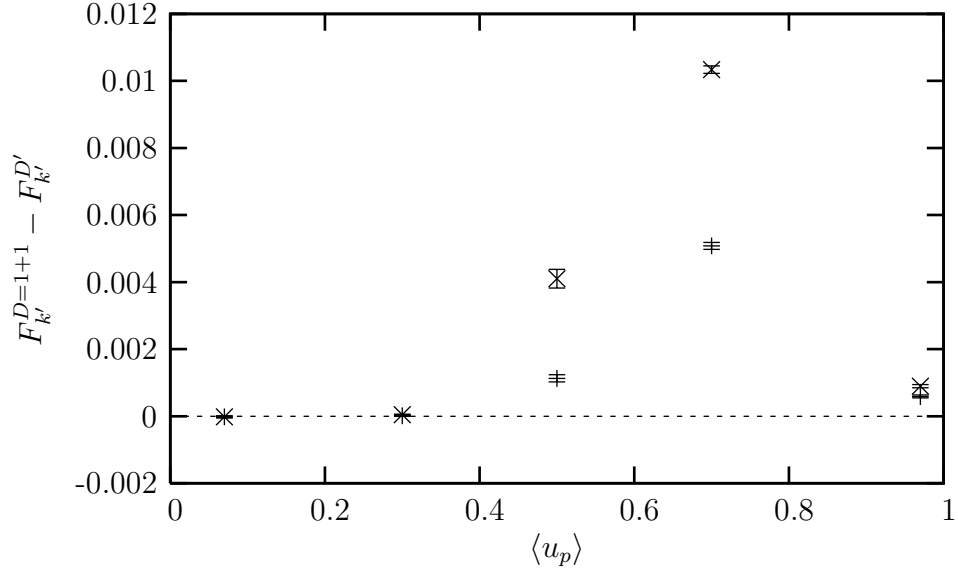


Figure 7: Difference between $F_{k'}$ in 1+1 dimensions and D' dimensions, for $D' = 2 + 1$ (+) and $D' = 3 + 1$ (x), as a function of the trace $\langle u_p \rangle$. All for the plaquette in $SU(3)$.

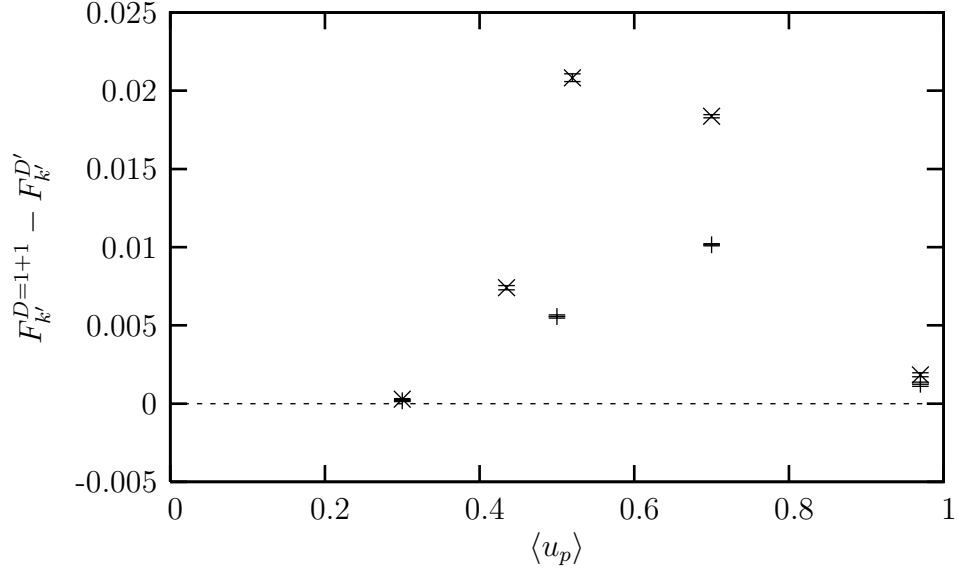


Figure 8: Difference between $F_{k'}$ in 1+1 dimensions and D' dimensions, for $D' = 2 + 1$ (+) and $D' = 3 + 1$ (x), as a function of the trace $\langle u_p \rangle$. All for the plaquette in $SU(6)$.

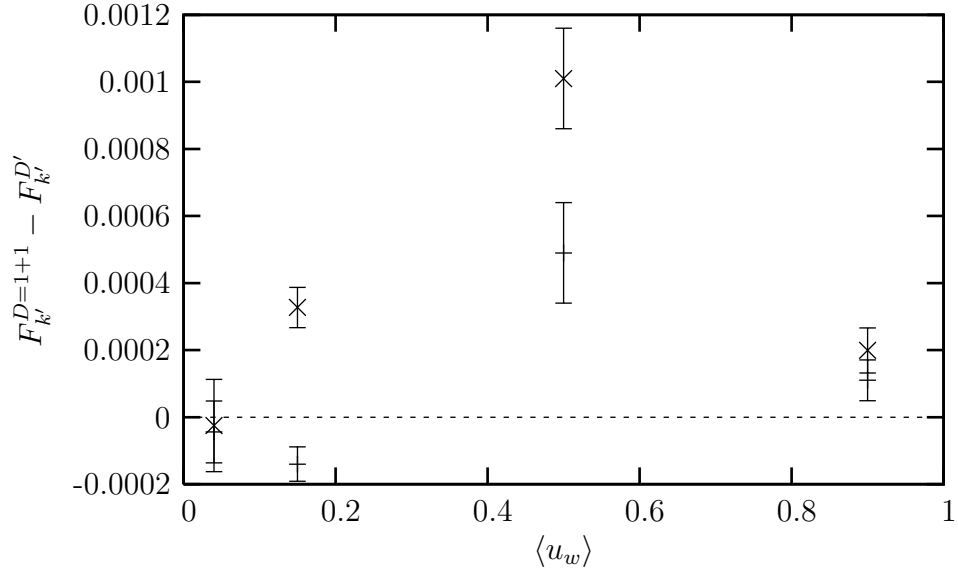


Figure 9: Difference between $F_{k'}$ in 1+1 dimensions and D' dimensions, for $D' = 2 + 1$ (+) and $D' = 3 + 1$ (x), as a function of the trace $\langle u_w \rangle$. All for the 2×2 Wilson loop in $SU(3)$.

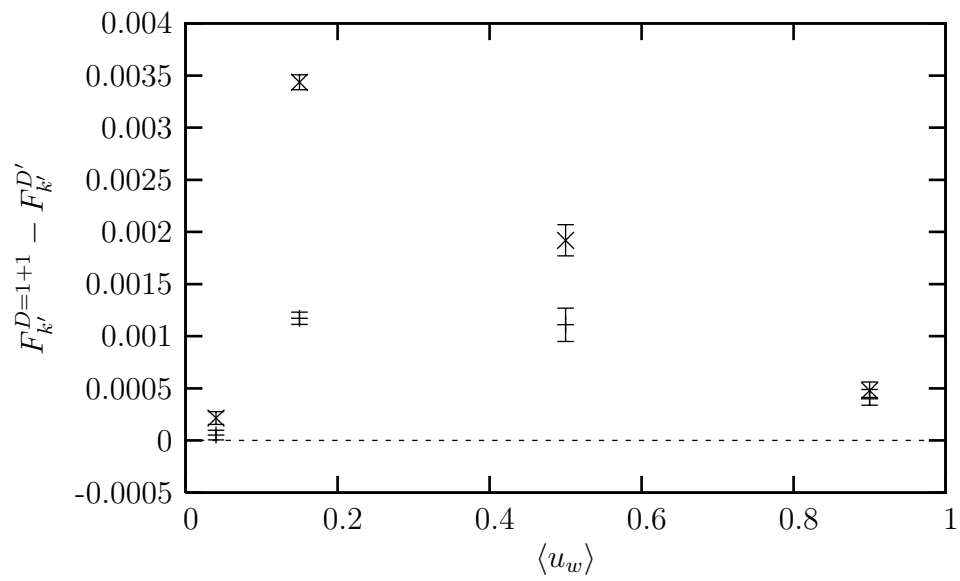


Figure 10: Difference between $F_{k'}$ in 1+1 dimensions and D' dimensions, for $D' = 2 + 1$ (+) and $D' = 3 + 1$ (\times), as a function of the trace $\langle u_w \rangle$. All for the 2×2 Wilson loop in $SU(6)$.